DEGREE PROJECT IN CHEMICAL ENGINEERING,
FIRST CYCLE, 15 HP
STOCKHOLM, SWEDEN 2022

High entropy oxide electrodes with ionic liquid electrolyte

SARON ABRAHAM

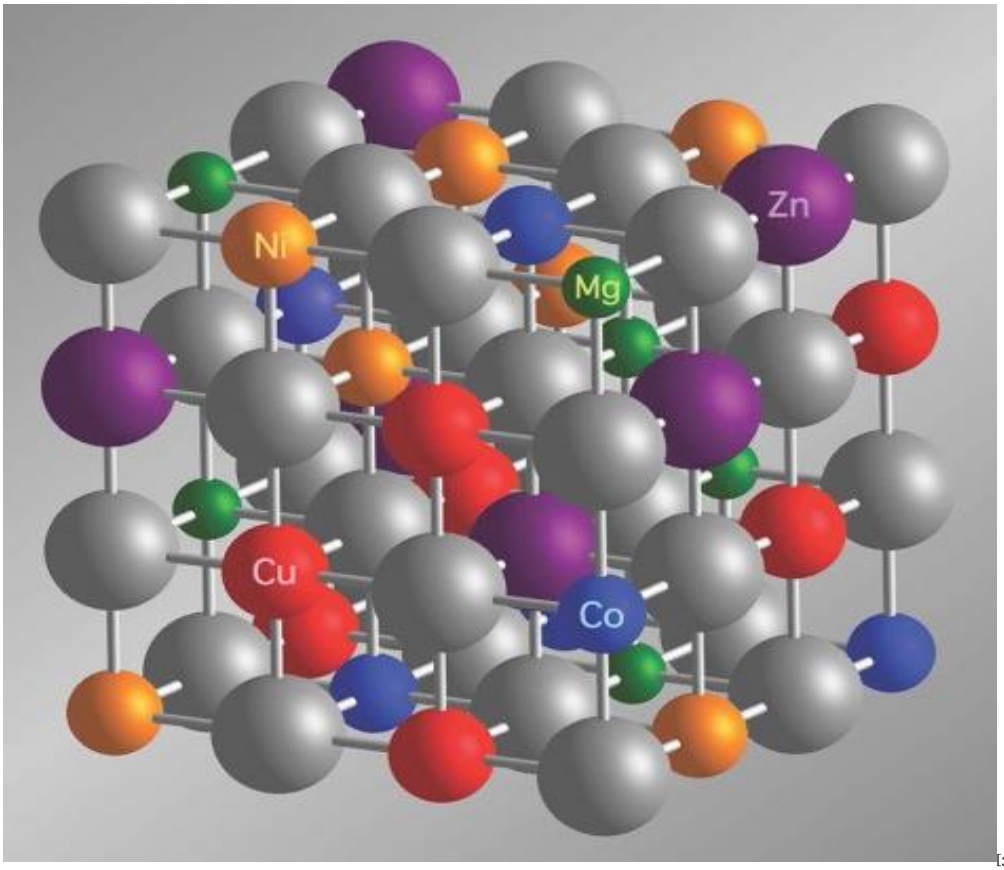

[34]

KTH ROYAL INSTITUTE OF TECHNOLOGY
SCHOOL OF ENGINEERING SCIENCES IN CHEMISTRY,
BIOTECHNOLOGY AND HEALTH

DEGREE PROJECT

Bachelor of Science in
Chemical Engineering

Title:	High entropy oxide electrodes with ionic liquid electrolyte
Swedish title:	Högentropioxidelektroder med jonisk vätskaelektrolyt
Keywords:	High entropy oxides, electrodes, Lithium batteries, ionic liquids, electrochemistry
Work place:	Division of applied physical chemistry, KTH
Supervisors at workplace:	Lilian Menezes de Jesus
	Aleksandar Tot
Supervisor at KTH:	Lilian Menezes de Jesus

Student:	Saron Abraham Tewelde

Date:	2022-06-08
Examiner:	James Gardner

Abstract

Metal-based high entropy oxides are considered promising electrode materials for use in Li-ion batteries. In this work, the most widely studied high entropy oxide $Mg_{0.2}Ni_{0.2}Cu_{0.2}Co_{0.2}Zn_{0.2}O$ (M-HEO) with rock salt structure was successfully synthesized by Modified Pechini synthesis, characterized by X-ray diffraction analysis, and investigated as anode active material (negative electrode) in a coin cell. M-HEO has the concept of entropy stabilisation of crystal structure in oxide system with the configurational entropy value of 1,6R which confirmed that M-HEO classified as high entropy oxide.

To test the electrochemical performance, full cells comprising M-HEO as anode, lithium manganese oxide (LMO) as cathode together with ionic liquid electrolyte were assembled to explore their potential for practical applications. The electrochemical cycling performance was studied by two electrochemical experiments which are three-electrode cyclic voltammetry and galvanostatic charge/discharge. The cyclic voltammetry measurement was used to determine the behaviour of the system such as potential window and scan rate, while galvanostatic charge/discharge was used to determine the performance of the battery over time by applying constant current.

The results demonstrate that high entropy oxide possess a stable structure. This points out the direction for the preparation of M-HEOs with stable structure and excellent performance and provides a promising candidate for anode materials for LIBs.

Keywords: Lithium-Ion Battery, High-Entropy oxides, Modified Pechini synthesis, X-ray diffraction, electrochemical performance

Sammanfattning

Metallbaserade högentropioxider anses vara lämpliga för användning av elektrodmaterial för litium-jon batterier. I detta arbete syntetiserades den första högentropioxiden $Mg_{0.2}Ni_{0.2}Cu_{0.2}Co_{0.2}Zn_{0.2}O$ (M-HEO) som har stensaltstruktur genom Modifierad Pechini-syntesmetod, karakteriserad av röntgendiffraktionsanalys och undersöktes som aktivt material i den negativa elektroden. M-HEO har konceptet av entropistabilisering av kristallstrukturen i oxidsystem som har det konfigurerade entropivärdet av 1,6R. Detta bekräftade att M-HEO klassificerades som högentropioxid.

För att testa den elektrokemiska prestandan, användes fullceller bestående av M-HEO som anod, litiummanganoxid (LMO) som katod tillsammans med jonisk flytande elektrolyt. Detta gjordes för att undersöka M-HEO potentiella praktiska tillämpningar. Den elektrokemiska cyklingsprestandan studerades genom två elektrokemiska experiment, cyklisk voltammetri med tre-elektroder och galvanostatisk laddning/urladdning med knapp-celler. Den cykliska voltammetri mätningen användes för att bestämma vart i systemet sker redox reaktion för att sedan kunna identifiera på vilka potentialintervall samt skanningshastighet, medan galvanostatisk laddning/urladdning användes för att bestämma batteriets prestanda över tid genom att applicera konstant ström. Resultaten visar sig att hög entropi oxider har en stabil stensaltstruktur. Detta bidrar till att M-HEO som har en stabil struktur kan vara ett lämpligt anodmaterial i litium-jon batterier.

Nyckelord: litium-jonbatteri, högentropioxider, Modifierad Pechini-syntes, röntgendiffraktion, elektrokemisk prestanda

ACKNOWLEDGEMENTS

I would like to thank my supervisors, Lilian Menezes and Aleksandar Tot, for their involvement and encouragement on my graduate work. I would also like to give thank my examiner for giving me this chance to do this project. I appreciate all the time I have spent with all of you discussing the project, results, and analysis.

I am grateful to all of those with whom I have had the pleasure to work during this project.

Table of Contents

1 Introduction

This section describes background to the project, its goals and purpose and limitations of the project.

1.1 Background

Developing new and advanced materials to meet future energy demands is one of the challenges in material technology [1]. One of the significant challenges is energy storage technologies such as developing new sustainable materials for Li-ion batteries [2]. In contrast to the other rechargeable batteries technologies (nickel-cadmium or nickel-metal-hydride), Li-ion batteries have advantages such as high energy densities, longer life span and low self-discharge rate [3]. Although Li-ion batteries can be an optimal choice for many renewable energy applications, they still have several drawbacks, especially with respect to safety that can lead to limitations on their performance [4]. These are the reasons why a constant hunt is needed for research on advanced materials for Li-ion batteries that exhibit properties that can be controlled.

The concept of high entropy materials is developing into a common term in materials research ever since emerging in the field of metallic alloys, which combine multiple elements in equimolar ratios by heating at a high temperature followed by quenching and these materials are called high entropy alloys [5]. By increasing the temperature, the entropy of configuration becomes dominates in the total Gibbs energy $\Delta G° = \Delta H° - T\Delta S°$. The high temperature is required in order to form a solid solution ($T\Delta S°$) and should be large enough to overcome a positive $\Delta H°$, which favors the formation of separate phases. Rapidly quenching the reaction by cooling it to room temperature is commonly performed to retain the high temperature solid solution and to avoid enthalpy-driven phase separation [2].

Rost et al. extend the “high-entropy” concept to oxides. By heating an equimolar mixture of Mg, Ni, Cu, Co and Zn binary oxides at high temperature followed by quenching, a $Mg_{0.2}Ni_{0.2}Cu_{0.2}Co_{0.2}Zn_{0.2}O$ (M-HEO) rock-salt structured solid solution was obtained. This material has the concept of entropy stabilization, which means stabilization of the resulting crystal structure, by increasing the configurational entropy of the resulting compound [6]. High-entropy oxides (HEOs) are made up of five or more metallic elements with similar ionic radii in stoichiometric proportions so that the configurational entropy $\Delta S_{config} \geq 1.5R$ per mole [1][5]. They are categorized as a new class of single-phase solid solution materials.

HEOs are relatively new multicomponent materials, one with promising futures in electrochemical applications [2] [6]. Since the first synthesized HEO, which has a rock salt structure and a chemical formula of $Mg_{0.2}Ni_{0.2}Cu_{0.2}Co_{0.2}Zn_{0.2}O$, they have been tremendously explored as electrode material for Lithium-ion batteries (LIBs) due to their unique electrical properties as well as a suitable alternative than the conventional electrodes [2].

In recent years, ionic liquid-based electrolyte has shown a potential application for Li-ion batteries. It’s due to their completely different physiochemical properties from other solvents such as organic carbonate solvents [15]. Their properties include non-flammability, high ionic conductivity as well as the properties of promoting the formation of stable SEI films [16].

In this project, it will be investigated by synthesizing the first HEO, $Mg_{0.2}Ni_{0.2}Cu_{0.2}Co_{0.2}Zn_{0.2}O$ (M-HEO) and testing the electrochemical performance in lithium-ion batteries that incorporate ionic liquid electrolytes. In order to make this work, both theoretical and experimental studies are involved to see the capacity of the M-HEO which is influenced by their basic properties as well as structural design. In order to investigate high entropy oxides, the paradigm of HEO which involves synthesis, structure, properties and performance is going to be covered.

1.2 Aim/Goals

The purpose of this project is to synthesize new-type of material called high entropy oxide, with composition $Mg_{0.2}Ni_{0.2}Cu_{0.2}Co_{0.2}Zn_{0.2}O$, and use it as an electrode together with ionic liquid electrolytes, in order to explore its use in the future lithium-ion batteries.

1.3 Research objectives

The general objective of the study is to investigate a high entropy oxide as electrode with ionic liquid electrolytes. To achieve these objectives, it is proposed:

- Synthesizing a high entropy oxide of the composition $Mg_{0.2}Ni_{0.2}Cu_{0.2}Co_{0.2}Zn_{0.2}O$ (M-HEO)
- Investigating the electrochemical properties of the M-HEO used as an electrode in Li-ion batteries, such as storage capacity and the cycling stability.
- Comparing a typical organic solvent-based electrolyte with the ionic liquid-based electrolyte with M-HEO electrodes.

1.4 Boundaries

These studies emphasize the importance of investigating materials as the negative electrodes in lithium-ion batteries in combination with an ionic liquid electrolyte. The electrochemical behaviour was tested with a coin-type cell. This project focused on a M-HEO with an equi-atomic ratio of metals in a single-phase rock salt high entropy oxide.

2 Theoretical Background

This chapter gives an overview of Li-ion batteries, high entropy oxides synthesis method, XRD and electrochemical measurements of electrode materials.

2.1 Lithium-ion battery

Lithium is used in batteries mostly because lithium is the lightest metal and also has good electrochemical potential. One of the most popular types of rechargeable battery is a lithium-ion battery where lithium ions move from the positive electrode to the negative electrode during charge and back when discharging. Many portable devices such as cell phones and laptop computers use Li-ion batteries due to their high energy density. The Li-ion batteries have the largest energy density compared to any other battery technology today [3]. The development of Li-ion batteries was investigated because of the safety concerns of lithium metal batteries. Even though Li-ion batteries have lower energy density than lithium metal, Li-ions are less reactive during charging and discharging steps than lithium metal batteries and

thus safer. However, there is always a place for making the Li-ion batteries more stable as well as safer by changing different components from the Li-ion battery. The commercial Li-ion batteries still tend to overheat and can be damaged at high voltages [3][5].

A Lithium-ion battery consists of one or more power generating units called cells that convert electrical energy to chemical energy [7]. A Li-ion cell consists of four main parts: the positive electrode, the negative electrode, a separator and an electrolyte. Every part is essential as a Li-ion battery cannot repeatably function when one of the components is not present. The active materials in a lithium ion battery consist of the positive and negative electrodes as well as the electrolyte. These active materials participate in the electrochemical charge and discharge reaction [8].

2.1.1 Electrodes

The most common electrochemical cell setups used in electrochemistry are three-electrode setup. The three-electrode setup is based on using three different electrodes; the working electrode, counter electrode and reference electrode where they differ by their geometric characteristics and placement. The working electrode is the most important component of an electrochemical cell where the redox reaction occurs. The counter electrode is an electrode which an electric current is expected to flow. It is ideally placed at a relatively large distance from the working electrode [9]. However, the reference electrode should be placed in close vicinity to the working electrode. This allows minimizing possible measurement errors such as effects related to the ohmic potential drop [10].

There are two types of working electrodes: the positive and negative electrodes. When naming the working electrodes, it is preferable to use the positive electrode and the negative electrode instead of referring to a cathode and an anode. It is because during charge and discharge of the battery, a cathode and an anode can be both positive or negative electrodes, i.e., the electrode with a higher potential is the positive electrode. During discharge, a cathode has higher potential which makes it a positive electrode. However, during charge, an anode has higher potential which makes it a positive electrode and the negative electrode would be a cathode [3][9]. The positive electrode of a conventional Li-ion cell uses an intercalated lithium compound as the material at the positive electrode is made from a metal oxide, the negative electrode is a carbon (graphite) [11].

The reference electrode has a fixed known potential for the purpose of measuring the potential of the working electrode without passing current through it. In Li-ion batteries, the reference cell provides a constant reference potential by making the lithium-ion activity constant. The counter electrode provides a means of applying input potential to the working electrode and the purpose is to complete the circuit and allow the current(charge) to flow through it. In Lithium-ion batteries, lithium metal is commonly used as a counter electrode [12].

2.1.2 Electrolyte

The electrolyte is one of the key components in lithium-ion batteries which requires good ionic conductivity and good chemical and electrochemical stability. Electrolyte allows the movement of ions only such as in Li-ion batteries; electrolytes allow Li-ion to move from one electrode to another electrode [13].

The electrolyte of a conventional lithium-ion battery is made up of a lithium salt in an organic solvent in solid or liquid form. Electrolyte formulations for Li-ion batteries typically consist of a conducting salt, (commonly lithium hexafluorophosphate ($LiPF_6$) dissolved in mixtures of linear (e.g., dimethyl carbonate (DMC), diethyl carbonate (DEC), ethyl methyl carbonate (EMC)) and cyclic organic carbonates (e.g., ethylene carbonate (EC) [13]. There are also more environmentally friendly as well as sustainable solvents called ionic liquids which will be discussed in the next chapter.

During the first charge and discharge cycles, commonly called formation cycles, interphases are formed. The first formation of interphase during the first cycles for a long-term performance of Li-Ion. The electrolyte salt and solvent molecule decomposition caused by electrochemical instabilities leads to a wide range of decomposition species contributing to the formation of performance-impairing side reactions [14].

2.1.2.1 Ionic liquid as electrolyte

One of the most sustainable electrolytes is ionic liquid which has attracted great attention. Ionic liquids are salts that have low melting point and are usually liquid at room temperature. One of the essential reasons why the application of ionic liquids growth is to the green chemistry movement. Many researchers describe ionic liquids as green solvent because they can contribute to more sustainable production because of their high thermal stability and a negligible vapor pressure. While other solvents like organic solvents can completely evaporate at high temperatures [15] [16].

Ionic liquids are used in many fields, one of the most potential applications is for energy generation and storage. Using them as electrolytes in batteries was one of the first applications considered when Chloroaluminate ionic liquids were discovered. Eventually the less reactive systems were introduced. The conventional Li-ion batteries which have a flammable organic solvent needed an immediate replacement. Since ionic liquids are non-volatile as well as non-flammable, it became a safer replacement for the organic solvent. The advantages of ionic liquids exceed within time including stability to different electrode materials, good discharge ability as well as satisfying cycle ability. For all of these advantages of ionic liquids as electrolytes make them fascinating, however, some problems show up such as high viscosity, ineffective mass and charge transport, while maintaining thermal and electrochemical stabilities. These problems require new possible candidate ions to be developed [15].

Ionic liquid can be used as solvents without being a component in a chemical reaction. The most common cations and anions used for ionic liquids are named on Figure 1 and 2. There are several cation-anion combinations that will give ionic liquids from which the ideal ionic liquid for any application can be selected [15].

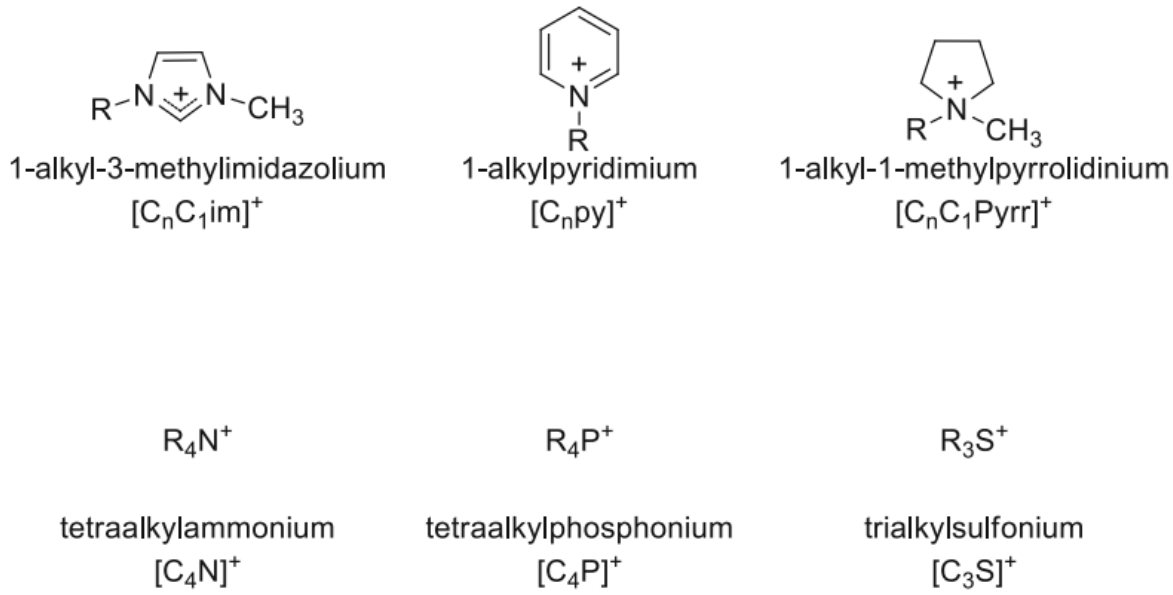

Figure 1. Commonly used cations for ionic liquids.

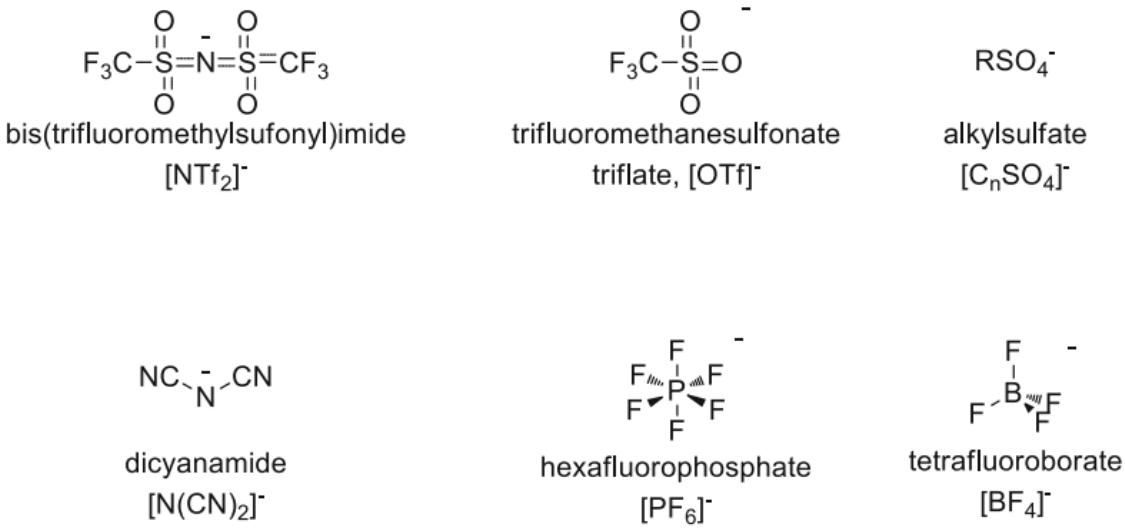

Figure 2. Commonly used anions for ionic liquids.

2.1.2.2 Solid electrolyte interface

On the negative side of the electrode during charge lithium ions are solvated by solvent molecules which approach the surface of the negative electrode material (usually graphite). The solvation leaves the lithium ion and get inserted into e.g. the graphite sheets, at that step the potential of the negative electrode is very low and there is a thermodynamic driving force

for electrolyte reduction. This is when the formation of the composition product that deposits on the surface. The product layer on lithium metal or on the electrode material (graphite) is called solid electrolyte interface (SEI) [14]. It's composed of different degradation products such as lithium- oxides, fluoride, carbonate or oligomers. The formation of the SEI layer negatively affects the battery because it's reversibly consuming lithium and electrons. However, the layer allows the battery to work by serving as a protection on the graphite electrode. The lithium ion can pass through it but not the electrons avoiding further degradation of the electrolyte and providing good efficiency of the battery. The nature of the SEI is influenced by several parameters such as the composition of the electrolyte, the nature of the electrode and its surface orientation [14].

When it comes to the positive electrode is generally a lithium layer oxide such as lithium cobalt oxide. There is no decomposition of the electrolyte through an electrochemical reaction on the surface of a positive electrode; however, some lithium carbonate and fluoride are detected on the surface of the positive electrode [13] [14].

2.1.3 The principle of Li-ion batteries

Energy is stored and released chemically in Li-ion batteries through redox reactions. Redox reactions occur in the electrodes where the electrode that accepts electrons is called the oxidant while the electrode that loses electrons is called the reductant [17].

In order to generate electric current, the lithium ions travel from the negative electrode through the electrolyte to the positive electrode during discharge. The movement of the lithium ions generate free electrons that travel though the external circuit. The separator blocks the short-circuiting of the battery. The separator also prevents contact between the positive and negative electrodes so that the battery will work properly [18].

During the charging process, lithium ions are released by the positive electrode and then go back to the negative electrode. When it's discharging, the electrochemical process is reversed. The electrolyte serves as the medium that enables the movement of lithium ions between the electrodes. For this to happen efficiently a large amount of lithium per unit weight storage needed on both anode and cathode [17].

The Li-ion needs to be able to move in and out of the cathode, the anode as well as through the electrolyte easily, the movement of receiving and releasing Li-ion easily is called ionic mobility. Once the ion passes through the electrolyte the electrons go around the conductive wire [18]. The flow of electrons produces an electric current that can be used to do work.
In order to have high power on the battery, the voltage difference between the electrodes has to be as high as possible [17].

2.2 Modified Pechini synthesis

In order to synthesize multicomponent complex oxide material modified Pechini synthesis became one of the most popular synthesis methods. This method is simple and straightforward as well as does not require complicated laboratory infrastructure facilities. There are three

major steps of the modified Pechini process in order to achieve a homogeneous oxide powder or film. These are aqueous solution of precursors, drying and heating of the solution and decomposition of the precursor material [19].

The first major step is making a stable aqueous chelated solution with the cation precursors, which has to be soluble in water with the chelating agent such as carboxylic acid. Chelating agents are used to prevent different interactions between metal ions present in the solution. The most common, highly soluble precursor for most metals is their nitrates. When multicomponent materials are being produced, it is important that the components, in this case the cations, are mixed in the correct stoichiometric ratio. The concentration range of the cations are typically from 0.1 to 1.0 M. The formation of chelate citric acid is used which is one of the most commonly used as a complexing agent as well as polybasic hydroxyl carboxylic acid. Typically, the carboxylic acid such as citric acid is added in excess, normally with a molar ratio of citric acid: cations from 1 to 3, and this ratio is important for the success of the synthesis. When it comes to the order of mixing the cations and chelation agents, it's favorable to add the cation forming the most stable chelate first and followed by the cations that form less stable chelates. After the formation of a chelate, the formation of polymerization is needed in order to promote homogeneity of the final oxide. For this to happen, the addition of a polyalcohol (usually ethylene glycol) with the polybasic carboxylic group gives the reaction a polyester product. The amount of ethylene glycol has to match or at least be the minimum amount as the esterification reaction [19].

The second major step is drying and heating of the solution obtained and forming a polymeric resin. In this step, it is important to prevent precipitation as the amount of water decreases. The whole reaction needs a heat treatment which leads to removal of excess water. In this step the solution is usually dried at temperatures in the range 110-150 ℃ [19].

The third step is thermal decomposition with high temperature treatment in order to decompose the precursor material to obtain an oxide powder. In this part, the organic part of the material will be removed. The polymeric resin can be produced with a higher temperature than the first step, usually between/below 400-500 ℃ depending on the components. This leads to an increase of volume which occurs due to release of water from hydrated chelates. After drying the method, the aqueous precursor solution becomes a brittle voluminous spongy-like precursor material. In some cases, after thermal decomposition, calcination takes place simply heating the material to create a powder of desired composition and structure [19].

2.3 X-ray diffraction

X-ray diffraction analysis (XRD) is an analytical technique designed to determine the crystallographic structure of the material including providing information about identification and quantification of crystalline phases [20]. One of the advantages of this analytical technique is, analyzing the purity of a crystalline sample without destructive the material. X-rays are generated by a cathode ray tube filter to produce monochromatic radiation to the sample [20] [21]. The interaction of the incident X-rays with the sample produces constructive interference when conditions stated in Bragg's Law are satisfied. Bragg's Law associated with the wavelength of the X-ray to the angle of diffraction and the crystalline sample of the lattice

spacing (see Equation 1). It states that when the X-rays is incident onto a crystal surface, its angle of incidence, θ, will reflect back with the same angle of scattering, θ. When the path difference, d is equal to an integer number, n, of wavelength, a constructive interference will occur [21].

Bragg's Law [22]

$$n\lambda = 2dsin\theta \quad (1)$$

where:

- λ is the wavelength of the x-ray [nm]
- d is the spacing of the crystal layers [nm]
- θ is the angle of incidence [degrees, °]
- n is an integer

The characteristic X-ray diffraction patterns generated in XRD analysis provide the fingerprint of the crystal structure present in the sample [21]. By comparing the standard reference patterns and measurements the fingerprints allow identification of the crystalline forms. The deflected diffraction pattern gives information as the distinguishing the phase, the size number of the crystal, classification and structure will be gathered [23].

A crystalline sample has different orientations of planes, depends on which direction the X-ray is getting its reflection, the planes are being mentioned with the help of miller indices Different planes are being mentioned with the help of hkl indices (Miller indices) [21] [23].

2.4 Scanning electron microscope (SEM)

SEM is used to see the microstructure and morphology of almost any material. The principle of SEM is that an electron beam is radiated to the material which helps to scan the surface of the material sample. As the electron beam with low energy reaches and enters the sample surface many interactions take place. As a result, electrons get emitted from or near the sample surface. By using different types of detector, an image is constructed from the signals which are produced from the electron sample interactions [24].

2.5 Electrochemical measurements of electrode materials

In order to optimize each electrode, it is not necessary to build a real electrochemical device (ex. Li-ion batteries), instead it's easier to study half-cell reactions that allows to best optimize each electrode by using potentiostat that conduct three electrode setups [25]. There are two variables in potentiostat; independent variable which can be voltage across working electrodes versus reference electrode (helps set up the voltage) and dependent variable that is current through working electrode [26].

Potentiostat has three major jobs; these are controlling voltage across working and reference, make sure there is no current going through reference and direct all current through the

counter. The result of an electrochemical experiment that can be performed with a potentiostat is called cyclic voltammetry [27].

Cyclic voltammetry is an electrochemical technique typically engaged to investigate the reduction and oxidation processes of molecular species. During measuring with cyclic voltammetry, the receiver produces a graph called voltammograms or cyclic voltammograms where the x-axis represents a parameter that is imposed on the system commonly, the applied potential (E), while the y-axis is the response which is commonly used the resulting current (i) passed [28]. In CV data IUPAC convention is mostly used convention where the oxidation is the highest curve, see the Figure 3.

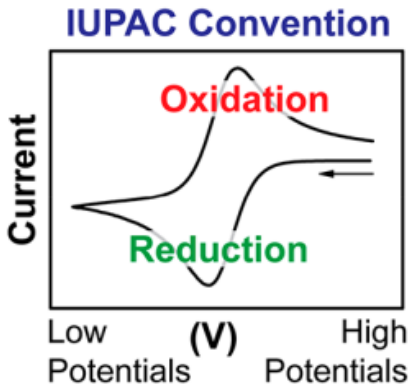

Figure 3. IUPAC convention [28].

In order to understand the "duck" shape(peaks) on the graph (Figure 3), Nernst Equation plays the main role, since the equation relates the potential of an electrochemical cell (E) to the standard potential of a species (E°) and the relative activities of the oxidized and reduced analyte in the system.

A cyclic voltammetry experiment uses a vessel called an electrochemical cell in order to measure the performance [29]. A schematic representation of an electrochemical cell is presented in Figure 4.

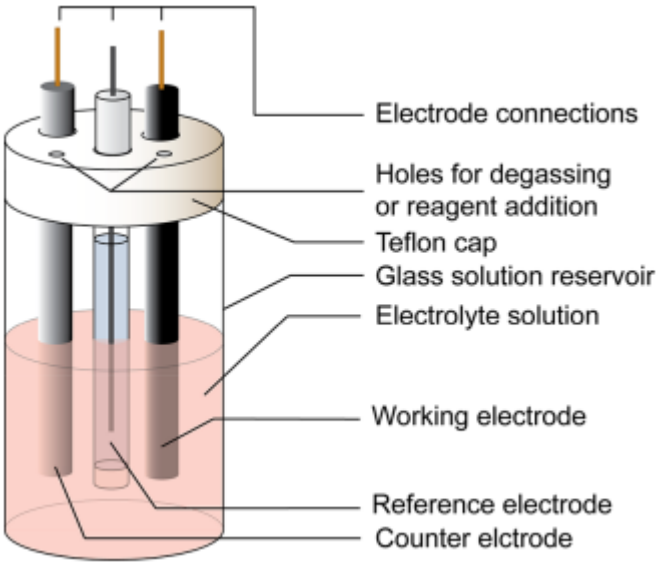

Figure 4. Schematic representation of an electrochemical cell for CV experiments [29].

2.6 Stabilization by configurational entropy

The concept of entropy stabilization is based on maintaining a single-phase structure by increasing the configuration of entropy of the system (for instance, solid material). This can be achieved by increasing in equimolar concentrations the elements of the system which are randomly distributed in a single lattice [30]. Depending on the entropy configuration ΔS_{config} values, solid materials are classified as low entropy(<1R), medium (1-1.5R), and high entropy(>1.5R) where are represent gas constant. In order to differentiate the types of materials, the value of ΔS_{config} can be calculated by using the following equation 2[31]:

$$S_{config} = -R\left[\left(\sum_{i=1}^{N} x_i ln x_i\right)_{cation-site} + \left(\sum_{j=1}^{N} x_j ln x_j\right)_{anion-site}\right] \quad (2)$$

Where x_i and x_j represent the mole fractions of cation- and anion-site respectively [30].

2.7 Capacity of a battery

One of the critical battery characteristics or specification is the capacity of the battery. Battery capacity is the energy/charge stored in a given battery and commonly measured by the unit ampere hours. The unit of ampere hour (Ah) defined as the number of hours for which a battery can provide a current equal to the discharge rate at the nominal voltage of the battery. Charging or discharging rates of battery has an impact on the rated battery capacity. When a battery discharged very quickly (meaning the discharge current is high), then the amount of energy that can be extracted from the battery is reduced which leads to lower battery capacity. This is because of the important components for the reaction to occur do not necessarily have enough time to either move to their necessary positions. In another word, only the fraction of the total reactant is converted to other forms, and therefore the energy available is reduced. On the other hand, when a battery discharged at a very slow rate (meaning the discharge current is low), more energy can be extracted from the battery and as a result the battery capacity is higher. That is why the battery of capacity should include the charging/discharging rate [32].

3 Methodology

This project took 10 weeks and was approached from two fronts; a literature review and experimental section which includes material synthesis, data analysis as well as experimental testing. The literature review consisted of a desk study based on evaluation published reports, scientific articles.

3.1 Experimental section

This section will present a description about how the high entropy oxide material was made, characterized as well as how electrochemical measurements were carried out.

3.1.1 Chemical reagents

The chemicals Ni $(NO_3)_2 \cdot 6H_2O$ (Sigma, 99.999%), Cu $(NO_3)_2 \cdot 3H_2O$ (Sigma, >99%), Co $(NO_3)_2 \cdot 6H_2O$ (Sigma, 99.999%), $ZnC_4H_6O_4 \cdot 2H_2O$ (Sigma, >99%), and $MgC_4H_6O_4 \cdot 4H_2O$ (Sigma, 99%) were the cationic precursors used in this work. In order to form a chelate a carboxylic acid (commonly, citric acid $C_6H_8O_7$) used with the cationic precursors, and in order to form a polyester the addition of a polyalcohol (commonly, ethylene glycol $C_2H_6O_2$) is needed.

3.1.2 Synthesis of HEO

The $Mg_{0.2}Ni_{0.2}Cu_{0.2}Co_{0.2}Zn_{0.2}O$ (M-HEO) powder was synthesized using the method called modified Pechini process. The starting materials are mentioned on Table 1 with respect to their stoichiometric amounts. Firstly, a chelate was formed between an aqueous solution (0.1g/ml) of citric acid ($C_6H_8O_7$) and the cationic precursors by combining them together in a 500 ml beaker. The beaker was placed on a hot plate, held at a temperature between 100-110 ℃, and stirred with a magnetic stir bar, this formed metals citrate. For the formation of a polyester(polymer) a polyalcohol (ethylene glycol $C_2H_6O_2$) was then added to the beaker. The mass ratios of the metals and citric acid were 1:3 while ethylene glycol with citric acid were 3:2, (see Table 1). The mixture gets heated for some minutes until everything is homogenized and has a transparent blackish color. Heating the solution on the hot plate helps to remove excess water. In order to remove the organic compound and form the starting powder, the solution was heated at 550 ℃ in the furnace for 5 hours with a heating rate of 2 ℃/min. The starting powder was then homogenized in mortar and calcined at 1000 ℃ for 2 hours with a heating rate of 8 ℃/min. The resulting M-HEO powder, was air quenched to room temperature.

Table 1. The starting salts in order to produced 5 g of M-HEO with their stochiometric masses.

Starting salts	Mass of the salts to calculated to yield the M-HEO [gram]
$Ni(NO_3)_2 \cdot 6H_2O$ (Sigma, 99.999%)	4.1467
$Co(NO_3)_2 \cdot 6H_2O$ (Sigma, 99.999%)	4.1501
$Cu(NO_3)_2 \cdot 3H_2O$ (Sigma, >99%)	3.4452
$ZnC_4H_6O_4 \cdot 2H_2O$ (Sigma, >99%)	3.1302
$MgC_4H_6O_4 \cdot 4H_2O$ (Sigma, 99%)	3.0581
Citric acid (C_6H_8O)	41.0945
Ethylene Glycol (C_2H_6O)	27.3963

3.1.3 Material characterization (XRD and SEM)

The crystalline structure of the prepared (starting and calcined) powders was analyzed by X-ray diffractometry at the operation voltage of 45 kV and current of 40 mA under Cu Kα radiation (λ = 1.54178 Å), and the diffraction angle (2θ) range between 15°–90°. The measurement required about 1 g sample. X-ray diffraction was carried out in both the starting powders annealed at 550 ℃ and the resulting powder which was calcined at 1000 ℃. The microstructure analysis of the powder calcined at 1000 ℃ were characterized using scanning electron microscope (SEM).

3.1.4 Preparing the electrode

For preparing a working electrode, three components; $Mg_{0.2}Ni_{0.2}Cu_{0.2}Co_{0.2}Zn_{0.2}O$ (M-HEO), carbon black and PVDF binder were mixed together with the mass ratio of 7:2:1. During optimization the mass ratio of 8:1:1 was also used see Table 2. The carbon powder improves conductivity while the binder holds the electrode material together. During mixing it is very important to homogenize(grind) the M-HEO and black carbon properly on the mortar. Afterwards, the PVDF binder, dissolved in 1-methyl-2-pyrrolidone, was added, and the resulting mixture was stirred in a vial sealed with parafilm to avoid volatilization of the solvent. The stirring was performed for about 4 hours in the initial tests and for 3 days in the optimized slurry, in order to get a homogenous consistency. The slurry product which is the working electrode was coated on both aluminum and stainless-steel foils and formed a film by using the doctor blade method. For this method, a glass slide was wiped with acetone as well as dropped some acetone on the glass slide in order to stick the current collector (aluminum and stainless-steel foils). After securing that the foil properly stuck to the glass slide and no more bubbles appeared from underneath the foil, the slurry poured on to the foil. The blade for the right amount of thickness (120 μm) dragged along the slurry surface, then left the coated

metal foil on the warm plate to dry before cutting and doing the measurements. Preparing M-HEO needed some optimizations by changing one factor at a time, such as changing the mass ratio of the components, amount of solvent (1-methyl-2-pyrrolidone), grinding and stirring time.

Table 2. shows different optimization mechanism by changing one factor at a time.

Mass ratio	HEO	Black carbon	PVDF	1-methyl-2-pyrrolidone	Grind the black carbon & HEO	Stirring time
8:1:1	0.2232 g	0.0279 g	0.279 g	1.0 ml	No grinding	4 hours
7:2:1	0.3 g	0.0857 g	0.429 g	1.5 ml	No grinding	4 hours
7:2:1	0.3 g	0.0857 g	0.429 g	1 ml	15 min	4 hours
7:2:1	0.3 g	0.0858 g	0.429 g	1 ml	30 min	3 days

3.1.5 Preparation of electrolyte

For this study, two types of electrolyte solvents were used. The first one is the most common electrolyte solvent which is an organic carbonate solvent (Dimethyl carbonate, DMC). The second one is an ionic liquid called 1-Methyl-1-propylpyrrolidinium bis(trifluoromethylsulfonyl)imide, [C_3Pyr] [TFSI]. The solute that has been used for both electrolyte solvent was bis(trifluoromethylsulfonyl)imide lithium salt, LiTFSI.

The electrolytes were prepared by mixing lithium salt and the solvents in a defined ratio. For the conventional electrolyte 1 M of LiTFSI dissolved in DMC. The same concentration of lithium salt dissolved in the ionic liquid. The solutions were preserved in small glass and used for several optimization electrochemical measurements.

3.1.6 Assembling the coin cells

Assembling the battery started with cutting out the working electrodes in a circular size from the current collector. To minimize edge defects during cutting, baking paper was used on the top of the electrode. The size of the working electrode had to be smaller than the counter electrode and both are smaller than the separator.

Firstly, the o-ring(spring) placed on the smaller cap then a spacer placed on the top of that. On the top of the spacer, the negative electrode placed and a small amount of electrolyte wet the negative electrode, a glass fiber separator placed on top as centered as possible then dropped some of the desired type of electrolyte. The amount of electrolyte in all coin cells was around 0.15 ml to fully wet the separators and electrodes. The positive electrode then placed and

closed the coin cell on the bigger can. The coin cell was then sealed using a crimping machine. The cap, can, spring and spacer are always a stainless-steel material while the rest is according to the following.

All the following materials used in order to assemble with two types of electrolyte coin cells:

- **Current collectors:**
  Aluminum foil
  Stainless-steel
- **Anode material (negative electrode):**
  M-HEO, carbon black and binder coated on both aluminum and stainless steel.
- **Cathode material (positive electrode):**
  Lithium manganese oxide (LMO) carbon black and binder coated on both aluminum stainless steel.
- **Electrolyte:**
  Conventional electrolyte: LiTFSI + DMC
  Ionic liquid: LiTFSI + [C_3Pyr] [TFSI]
- **Current collectors:**
  Aluminum foil
  Stainless steel
- **Coin cell type battery parts:**
  Stainless steel cap and gasket
  Stainless steel spring
  Stainless steel spacer
  Anode material
  Glass fiber separator
  Cathode material
  Stainless steel can

Table 3 shows detailed information about the assembling the coin cell in order to differentiate during charge/discharge measurements. The first two-coin cells ($1Al^{HEO}$ and $2Al^{HEO)}$ were assembled with the typical organic electrolyte solvent DMC while the third ($3Al^{HEO)}$ and the fourth ($4Al^{HEO}$) were tested with an ionic liquid [C_3Pyr] [TFSI]. In order to calculate the specific capacity of the battery the mass of electrodes was needed (see Table 3).

Table 3. assembling of four different coin cells with two different electrolytes and different masses of electrodes.

Coin cell labelled as	Mass of anode (HEO:Carbon black:PVDF) [gram]	Mass of cathode (HEO:Carbon black:PVDF) [gram]	Electrolyte	Assembling and measument day and time
$1Al^{HEO}$	0.0055	0.0072	LiTFSI + DMC	Assembled: 2022-05-18 at 11:00 Tested: 2022-05-18 at 13:00
$2Al^{HEO}$	0.0061	0.0066	LiTFSI + DMC	Assembled: 2022-05-19 at 10:00 Tested: 2022-05-19 at 11:00
$3Al^{HEO}$	0.0059	0.0070	LiTFSI + $[C_3Pyr]$ [TFSI]	Assembled: 2022-05-18 at 11:00 Tested: 2022-05-20 at 13:30
$4Al^{HEO}$	0.0062	0.00694	LiTFSI + $[C_3Pyr]$ [TFSI]	Assembled: 2022-05-20 at 13:50 Tested: 2022-05-23 at 08:30

3.1.7 Electrochemical measurements

The electrochemical measurements performed using an Autolab electrochemical workstation (Muti Autolab/PG12) at room temperature. Firstly, cyclic voltammetry was performed where the electrolyte solution was first added to an electrochemical cell and the three electrodes. The three-electrode (working-, reference- and counter electrode) CV test of M-HEO and moisture content measurements performed in glass-bottle-like cells. The HEO electrode was pre-coated on an aluminum current collector as thin film. The counter electrode(platinum) and Ag/AgCl reference electrode positioned in the glass as shown in Figure 4. After assembling the cell, the electrodes were connected to the potentiostat and the experimental parameters were selected according to Table 4 through the Nova 2.1 software software.

Table 4. shows the fundamental experimental parameters for the cyclic voltammetry and the exact values of each parameter.

Start- and stop potential	0 V
Upper vertex potential	3 V
Lower vertex potential	-3 V
The scan rate	0.05 V/s
The number of segments/scans	50

After assembling the coin cells, the Chrono discharge/charge galvanostatic test conducted also at the Autolab electrochemical workstation (Muti Autolab/PG12) at room temperature. The cycling procedure consists in a series of charge-discharge galvanostatic cycles in between 0 v to 3.0 V. The charge and discharge measurements were performed with the constant current density (120 mA/g). The current density was calculated from applied current and mass of active material was calculated as: (The mass of anode – The mass of non-coated current collector) * The proportion of the active material = The mass of active material.
Coulombic efficiency (CE) was also calculated as the following equation. The result will be presented in the next chapter.

$$CE = \frac{Chrage\ delivered\ during\ dischage}{Chagre\ stored\ during\ previous\ charge} \quad (3)$$

It was possible to compare the theoretical capacity and the practical specific capacity of an operating cell. The theoretical capacity of a cell can be calculated by using Faradays' law (see equation 4).

$$Q_{theoretical} = \frac{n*F}{3600*Mw}\ [mAh/g] \quad (4)$$

Where n is the number of charge carrier, F is the Faraday constant and Mw is the molecular weight of the active material used in the electrode.
The practical/experimental specific capacity can be calculated as the following equation:

$$Q_{experimental} = \frac{\int I*dt_{cutoff}}{\Delta V*m} \quad (5)$$

Where, I is the applied current, dt_{cutoff} is the time for fully charge and discharge battery (in hours), m is mass of the active material.

4 Results

4.1 Structure and microstructure characterization of the $Mg_{0.2}Ni_{0.2}Cu_{0.2}Co_{0.2}Zn_{0.2}O$ particles

Figure 5 illustrates the X-ray diffraction patterns of the starting powder particles (annealed at 550 ℃) which include rock salt, spinel, wurtzite and tenorite structures. The resulting powder particles confirmed that the synthesized powder exhibited a single phase (rock-salt structure) after calcination at 1000 ℃ for 2 h, followed by air quenching.

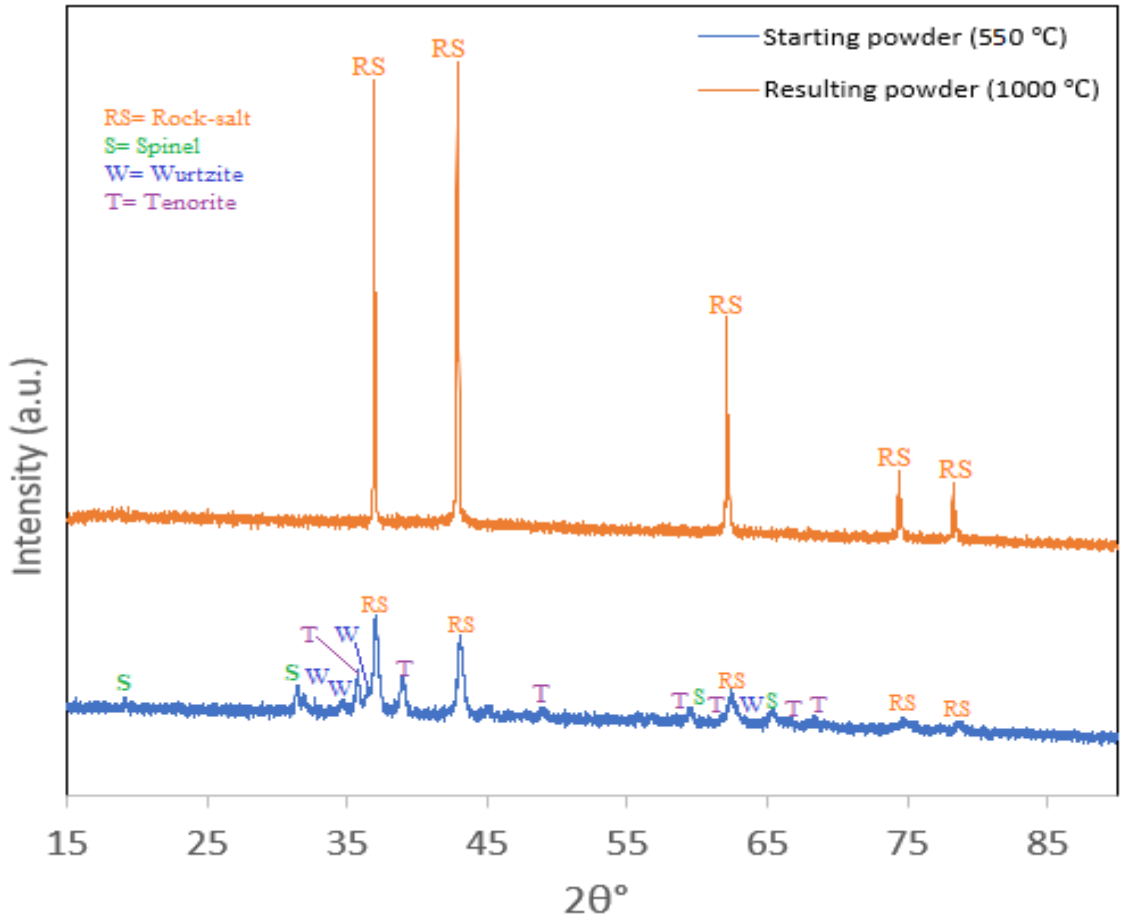

Figure 5. XRD of the starting powder (annealed at 550℃) and the resulting powder (calcinated at 1000℃)

Figures 6 and 7 show the morphology of $Mg_{0.2}Ni_{0.2}Cu_{0.2}Co_{0.2}Zn_{0.2}O$ particles via scanning electron microscopy (SEM) with two different scale bars. The scale bar on Figure 6 corresponds to 10 µm while the one in Figure 7, to 20 µm. The images show the variety of particle morphologies and sizes. Some of the particles are larger in size than the others. Furthermore, the particles are agglomerated as both figures are showing how materials stick together and form clumps.

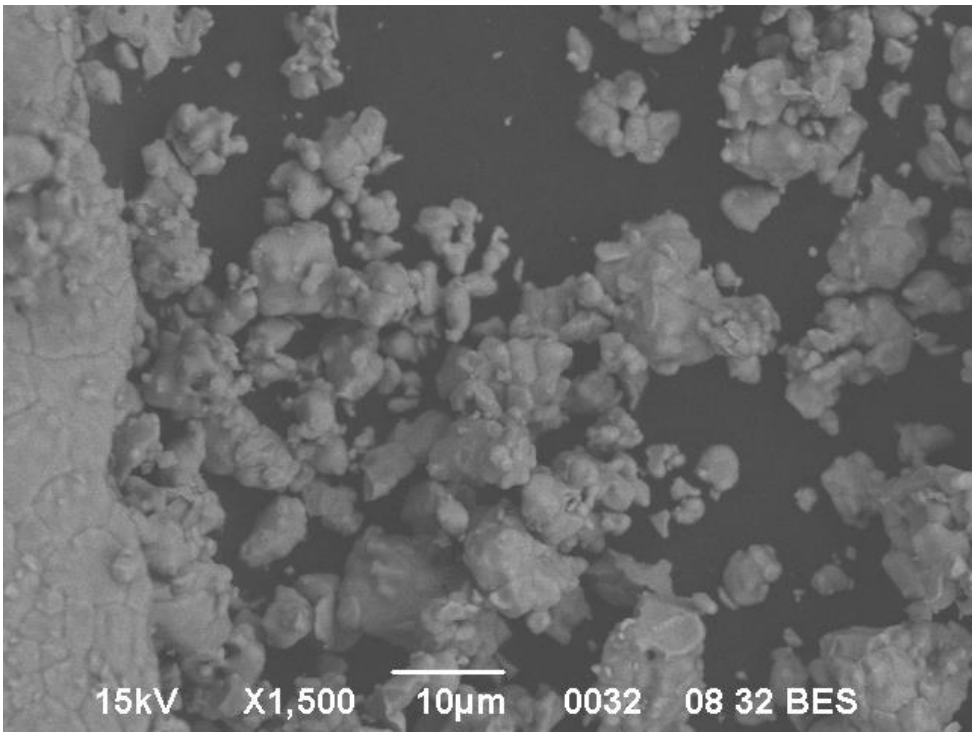

Figure 6. SEM image 10 µm.

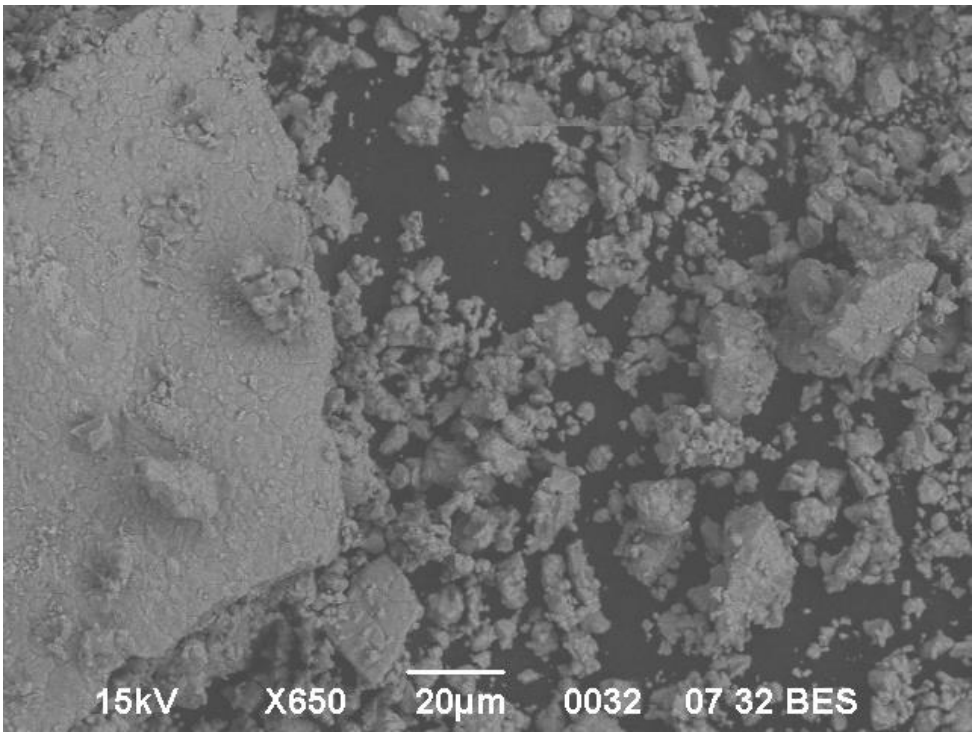

Figure 7. SEM image 20 µm.

4.2 Electrochemical performance studies of HEO

Cyclic voltammetry studies on $Mg_{0.2}Ni_{0.2}Cu_{0.2}Co_{0.2}Zn_{0.2}O$ electrodes were carried out at the scan rate of 0.05 V s^{-1} in the voltage window from -3 to 3 V vs. Ag/AgCl at room temperature. Pure platinum metal was used as the counter cell while Ag/AgCl as reference electrode. Figure 8 shows the CV curves using the conventional electrolyte.

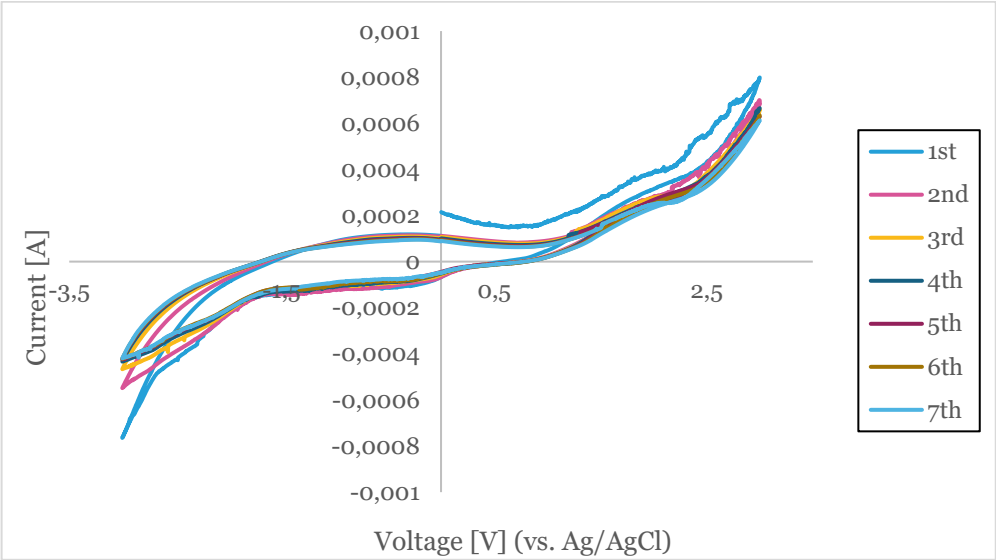

Figure 8. Representative cyclic voltammetry (CV) curves at a scanning rate of 0.05 V/s in the voltage range of -3 to 3 V versus Ag/AgCl.

Galvanostatic cycling studies were carried out on coin cell that was labeled as $3Al^{HEO}$on Table 3 (with ionic liquid). The electrochemical properties of the $Mg_{0.2}Ni_{0.2}Cu_{0.2}Co_{0.2}Zn_{0.2}O$ electrode in $3Al^{HEO}$ coin cell was determine in the voltage range from 0 V to 3 V. Figure 9 summarizes the cyclic performance where 10 cycle of charge and discharge measured. the capacity increase with each cycle.

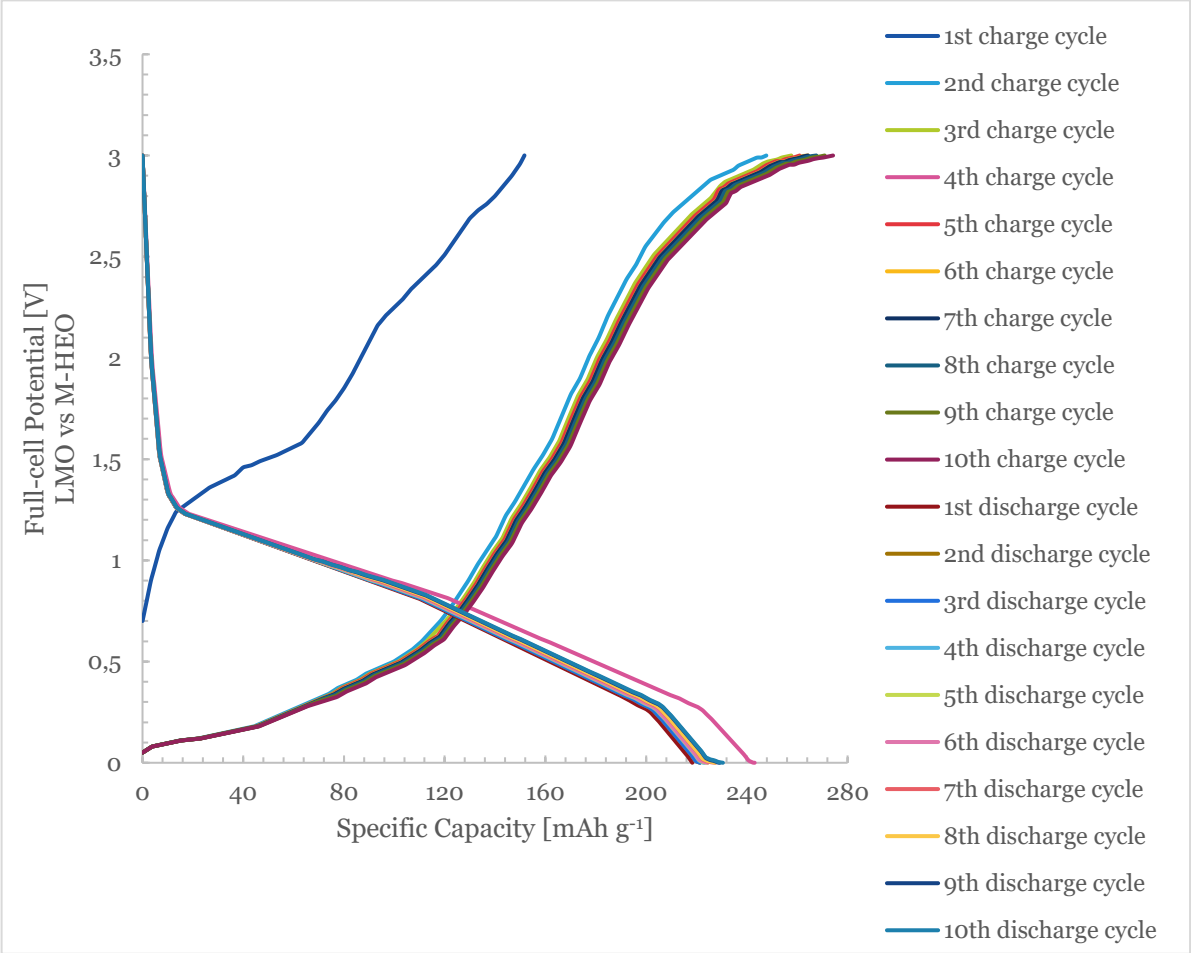

Figure 9. 10 cycle charge/discharge profile of a coin-type full-cell.

From Figure 10, 1st charging process was significantly faster, and one of the main reasons is the charging of battery before the measurements with each further cycle it can be noted that specific capacity for charging is continuously increasing. On the other hand, uniform trend of discharge process could not be clearly observed.

The Coulombic efficiency as well as the change of specific capacity during the cycling is presented in Figure 10. As can be also seen from Figure 10, the charge capacity increased during the time, while the discharge capacity is almost constant. Therefore, the coulombic efficiency was decreasing during the cycling.

The coulombic efficiency calculated to around 0.86. The theoretical capacity calculated to 382 mAh ¯g while the practical capacity estimated 259 mAh ¯g according to the voltage-time curve from the galvanostatic cycling test.

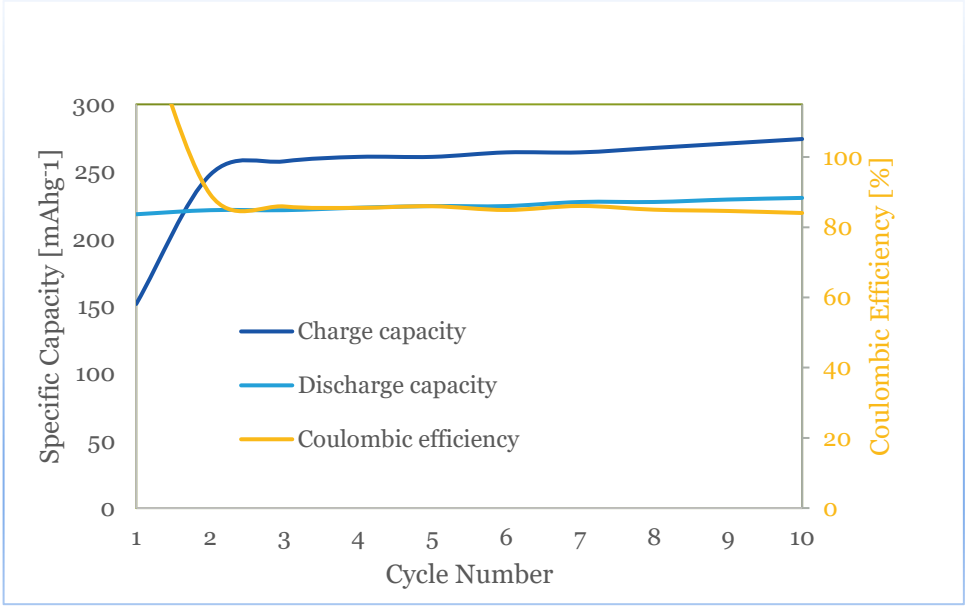

Figure 10. cycling performances and CEs of M-HEO// LMO coin cell with ionic liquid electrolyte.

5 Discussion

Here is the discussion of the results and methods which emphasize on comparing the pioneering paper.

5.1 Synthesizing HEO

The cation precursors used in this study as well as the synthesis mechanism (modified Pechini synthesis) were not the same as the ones used in the previous pioneering paper. However, $Mg_{0.2}Ni_{0.2}Cu_{0.2}Co_{0.2}Zn_{0.2}O$ (M-HEO) sample obtained after air-quenching from 1000 ℃ was single phase with a rock-salt crystal structure (see Figure 5). It is therefore shown that the modified Pechini synthesis is an effective method for producing the M-HEO. This method is simple and does not require complicated laboratory infrastructure facilities. The configurational entropy of M-HEO compound was calculated and it is presented in Appendix 1. When the configurational entropy of a material is higher than 1.5 R (where R represents gas constant), this material is considered a high entropy oxide [31]. The configuration entropy of the M-HEO was calculated to be1.61R. For that reason, M-HEO belongs to the high entropy oxide classification.

5.2 Characterization

The phase purity and crystallinity of the high entropy oxide $Mg_{0.2}Ni_{0.2}Cu_{0.2}Co_{0.2}Zn_{0.2}O$ were examined by X-ray diffraction technique (XRD). The starting powder was tempered at 550 ℃, lower temperature than the resulting powder which makes ZnO and CuO stable at 550 ℃ and present as wurtzite and tenorite structures respectively. MgO, NiO and CoO crystallizes in the rock salt structure. The XRD pattern of the starting powder has also reflections of spinel, which is related to Co_3O_4. To obtain the final single-phase rock-salt powder, a higher temperature was applied to the system. The calcinated sample at 1000 ℃ can be recorded as a single-phase, rock-salt structure along with the space group of Fm-3 m in agreement to JCPDS Card No 03-065-2901. The diffraction peaks detected at 2θ values of 36.9, 42.8, 62.1, 74.3 and 78.2° correspond, respectively, to the reflections of (111), (200), (220), (311) and (222) planes of a rock-salt structure. Besides no impurity peaks are detected, indicating the high purity of the rock-salt structured materials. The lattice parameter obtained from the Braggs' law of the XRD pattern was 4.22 Å, which is similar to the value reported by Bérardan D (4.24 Å) [33].

5.3 Preparing the electrode

To prepare a homogenous electrode slurry for the purpose of making a good film with M-HEO, four conditions were applied for optimization. In the first one a 8:1:1 mass ratio of M-HEO, carbon and PVDF was used. After applying the slurry on the aluminium foil using the doctor blade, the coverage was not homogeneous as it can be seen in Figure 11. Therefore, in the next experiments, the amount of the conductive agent (carbon) was increased, and the ratio of the slurry was set to 7:2:1 which was also used in Ref [1]. Furthermore, 0.5 ml of extra solvent was added to the mixture compared to the previous test to improve the mixing. However, the result became an unwanted consistency (due to excess solvent). Despite that, using different amounts of solvent is not necessary since the solvent will dry out later if the slurry when drying the coated electrode. As long as the solvent helps to homogenize all the powders uniformly.

The third and the fourth trial have the same amount of the composition but have different stirring time where the fourth trial has much longer time (3 days). The stirring time for the third trial was 4 hours and gave better consistency than the first and second one, it is assumed that grinding the black carbon and M-HEO was favourable. The fourth trial had the best consistency of all trials and used for the electrochemical measurements. In conclusion, leaving the mixture of electrodes for stirring for a longer time gives an optimal product for coating the slurry onto metal foil. It is also preferable to grind the black carbon and M-HEO on the mortar for a longer time since the two powders come with different particle sizes.

The consistency of the slurry is important to ensure a homogenous coverage of the metal foil. To get the desired consistency, grinding the M-HEO and the black carbon together and most importantly the stirring time for making the slurry was important. Longer stirring time was the main factor for the best slurry consistency, likely due to the agglomerated particles observed in SEM.

When it comes to the current collector, after some optimization, it was favourable to test the M-HEO material with aluminium current collector instead of stainless steel which was showing an overload of current.

Figure 11. Slurry of M-HEO electrode on aluminum foil.

5.4 Preparation of electrolyte

Before choosing the candidate ionic cation liquid, three different ionic cation liquids were tested. The testing mechanism involved mixing the high entropy oxide powder with each one of them and leaving them over the weekend. Despite that HEO did not react with any of them, so all of the ionic cations can be selected for the purpose of making the electrolyte with the lithium salt and testing their electrochemical performance with the assembled coin cell. However, because of lack of time, only one of the ionic cation liquids which was less viscous than the others were chosen.

According to the previous studies, the carbonate organic solvent is highly volatile and flammable, and when the temperature of the battery is higher, the lithium salt can suffer from thermal instability. However, for the purpose of providing a comparison study with the ionic liquid, a combination of Lithium bis(trifluoromethylsufonlysulfonyl)imide (LiTFSI) and

oxidatively stable dimethyl carbonate (DMC) has been used assuming the mixture enables the reversible intercalation of Li^+ ions into HEO anodes. As a result, while testing on this conventional mixture of electrolyte, the charge and discharge measurement was not working as expected.

5.5 Assembling the coin cell

In this work, CR2023 coin cell cases that are 20 mm in diameter were used. During cell assembly, the separator had to be much bigger than the electrodes so that it blocks any contact between the electrodes. It is necessary to fill enough electrolyte into the coin cells to moisten all pores, especially on the separator. Since the ionic liquid was more viscous than the carbonate-based solvent (DMC) electrolyte a little bit more electrolyte was used. In addition to, the resting time for the coin cell using ionic liquid before measurements was prolonged, to allow the separator get wet properly. Another thing to think about is crimping the coin cell well and the amount of pressure applied on the coin cell.

5.6 Electrochemical measurement

During collecting the data on a cyclic voltammetry Ag/AgCl took as the reference electrode. According to the previous pioneering paper, Li/Li^+ used as a reference electrode. To compare this research with the pioneering paper (see Ref [1]), the cyclic voltammetry data had to convert to potential with respect to lithium which has -3.04 V. The electrode potential of Ag/AgCl is 0.1976 and the difference of Li and Ag/AgCl is 3.237 V. To obtain the redox potential relative to a Li electrode, 3.237 is subtracted from all the potential. However, the cyclic voltammetry that was presented on Figure 12 does not only contain the calibrated value as the previous pioneering paper. Instead tested with the voltage range of -3 to 3.

To seeing the performance of new materials in Li-ion batteries, it was tested with hand-made full coin-type cells with M-HEO as the negative electrode and lithium manganese oxide as the positive electrode. A full cell would give more accurate data of the performance of active materials in the actual Li-ion batteries.

When it comes to the current collector, after some optimization, it was favourable to test the M-HEO material with aluminium current collector instead of stainless steel which was showing an overload of current while testing the electrochemical performance. There was an issue with crimping the stainless-steel with enough pressure, since the thickness of stainless steel was significantly lower. Therefore, it was possible to have air trapped in the battery that caused an issue while measuring with stainless-steel.

After assembling the coin cell with DMC-based electrolyte, linear sweep voltammetry was used to see if the coin cell was working since it was the fastest way to use. Linear sweep voltammetry was working while using the DMC-based electrolyte. However, it was not possible to test the charge and discharge of lithium-ion battery while using DMC-based electrolyte. It was then impractical to compare with the ionic liquid electrolyte. Although, it was possible testing the ionic liquid electrolyte, which shown presentable result.

Two cells were assembled with ionic liquid ($3Al^{HEO}$and $4Al^{HEO}$; see Table 3) to analyze simultaneously by checking the measurement reproducibility. In spite of that, there was

shortage of time therefore, at best one of the coin cell ($3Al^{HEO}$) was tested. The result will discuss in the next paragraphs.

Galvanostatic cycling studies carried out on $3Al^{HEO}$ coin cell to determine electrochemical properties of the $Mg_{0.2}Ni_{0.2}Cu_{0.2}Co_{0.2}Zn_{0.2}O$ electrode. The shape of the discharge and the charge curves gave information about the reversibility of the electrode reaction. The result shows that the specific capacity increases with each charge and discharge cycle. Figure 13 shown that the first and second charge/discharge cycle of a coin cell which did not achieved a large specific capacity in the first cycle, however a large specific capacity of about 248 $mAhg^{-1}$ was achieved in the second charge cycle. Note that the capacity was calculated based on the weight of M-HEO. A first cycle specific discharge capacity of 217 $mAhg^{-1}$was achieved, with an average discharge voltage of 2.65 V.

To describe the released battery capacity, coulombic efficiency was calculated (see appendix 1). Coulombic efficiency is the ratio of the discharge capacity after the full charge and the charging capacity of the same cycle. The cell has an average coulombic efficiency of 86 % and cycled stably for 10 cycles. The coulombic efficiency of Li-ion is normally better than 99 %. For this research, the low coulombic efficiency is due to the viscosity of the ionic liquid electrolyte, the compatibility of HEO electrode and LMO as well as the amount of active material on each electrode and the amount of electrolyte. It might also be due to electrode and electrolyte interactions with impurities, non-self-limited solid electrolyte interface or other parasitic pathways dependent on the electrode/electrolyte chemistries and the cycling parameters used when testing the cell. Although, 86 % for the coulombic efficiency is a promising result and the future investigation should be performed in order to optimize the battery system.

The theoretical capacity ($Q_{theoretical}$) of the cell also calculated (see Appendix 1) to compare it with the practical specific capacity. In this work, it was assumed that the number of charge carrier (n) in the Faraday's law equation (see Equation 4) was 1 (*further discussion continues below)*. The theoretical capacity for this case obtained to 382 $mAh^{-}g$. The practical specific capacity ($Q_{practical}$) calculated by the voltage-time curve that was obtained while testing $3Al^{HEO}$ coin cell from the galvanostatic cycling test. The practical capacity was obtained to 259 $mAh^{-}g$. The reason why practical capacity is lower than the theoretical capacity is that not all the Li ions can be removed from or inserted into the active electrode material.

The reactions that are occurring during the redox processes in this work is unknown since there might be additional processes might allow metals from M-HEO composition to form intermetallic phases. This leads to the number of charge carrier might not be Li-ion. According to this, the number of charge carrier assumed as the highest charge of the M-HEO composition which is 2. This also leads to the theoretical capacity of M-HEO compound cannot predict with high accuracy.

On Figure 10, the coulombic efficiency in the initial cycle was more than 100 %, the reason behind that, most likely lithium ions didn't have enough time to reach maximum occupancy in the electrode surface and its structure. Also, the starting potential was already higher, so that the charge process happened faster. However, in the subsequent cycles, the coulombic efficiency stabilized at about 84-87%.

6 Conclusions and outlook

In conclusion, high entropy oxide $Mg_{0.2}Ni_{0.2}Cu_{0.2}Co_{0.2}Zn_{0.2}O$ (M-HEO) with rock salt structure has been successfully synthesized by Modified Pechini synthesis method and exploited as negative electrode material in full cell with coin-type cell with lithium manganese oxide as a positive electrode. The average coulombic efficiency obtained to around 86 %. It was unable to predict the theoretical capacity since the reaction occurring during redox was unknown. According to this, future work should address the question of what the reactions are occurring during the redox processes in the case of M-HEO. Further work should also investigate the effect of different types of ionic liquid electrolytes with M-HEO. This work can be concluded that M-HEOs are the candidate negative electrodes for Li-ion batteries.

7 Reference

[1] Sarkar A, Velasco L, Wang D, Wang Q, Talasila G, de Biasi L, et al. High entropy oxides for reversible energy storage. Nat Commun [Internet]. 2018 [cited 2022 Apr];9(1):3400. Available from: https://www.nature.com/articles/s41467-018-05774-5

[2] Qiua N, Chenab H, Yang Z, Sun S, Wang Y, Cui. Y. A high entropy oxide (Mg0.2Co0.2Ni0.2Cu0.2Zn0.2O) with superior lithium storage performance [Internet]. Sciencedirect.com. 2019 [cited 2022 Mar]. Available from: https://www.sciencedirect.com/science/article/pii/S0925838818341677#fig4

[3] Lithium-ion battery [Internet]. Clean Energy Institute. 2015 [cited 2022 Apr]. Available from: https://www.cei.washington.edu/education/science-of-solar/battery-technology/

[4] Gregus N. 4 benefits of lithium-ion batteries [Internet]. EnergyLink. 2021 [cited 2022 Apr]. Available from: https://goenergylink.com/blog/4-benefits-of-lithium-ion-batteries/

[5] Musicó BL. Synthesis and Physical Properties of High Entropy Oxide Ceramics [Internet]. Tennessee.edu. 2021 [cited 2022 Apr]. Available from: https://trace.tennessee.edu/cgi/viewcontent.cgi?article=7836&context=utk_graddiss

[6] Berardan D, Meena A, Franger S, Herrero C, Dragoe N. Controlled Jahn-Teller distortion in (MgCoNiCuZn)O-based high entropy oxides [Internet]. Sciencedirect.com. 2017 [cited 2022 Apr]. Available from: https://www.sciencedirect.com/science/article/pii/S0925838817304863

[7] Lithium ion batteries (LI-ION) [Internet]. Energy Storage Association. 2019 [cited 2022 Apr]. Available from: https://energystorage.org/why-energy-storage/technologies/lithium-ion-li-ion-batteries/

[8] Paravasthu R, James SP, Prieto A, Wu M. SYNTHESIS AND CHARACTERIZATION OF LITHIUM-ION CATHODE MATERIALS IN THE SYSTEM (1-x-y)LiNi 1/3 Mn 1/3 Co 1/3 O 2 • xLi 2 MnO 3 • yLiCoO 2 submitted by [Internet]. Mountainscholar.org. [cited 2022 Apr]. Available from: https://mountainscholar.org/bitstream/handle/10217/65349/Paravasthu_colostate_0053N_11081.pdf?sequence=1

[9] Costard J, Ender M, Weiss M, Ivers-Tiffée E. Three-electrode setups for lithium-ion batteries: II. Experimental study of different reference electrode designs and their implications for half-cell impedance spectra. J Electrochem Soc [Internet]. 2017;164(2):A80–7. Available from: http://dx.doi.org/10.1149/2.0241702jes

[10] Ohmic drop [Internet]. PalmSens. [cited 2022 Apr]. Available from: https://www.palmsens.com/knowledgebase-topic/ohmic-drop/

[11] Vetter J, Wohlfahrt-Mehrens M. SECONDARY BATTERIES – LITHIUM RECHARGEABLE SYSTEMS – LITHIUM-ION | Aging Mechanisms [Internet]. Sciencedirect.com. 2009 [cited 2022 Apr]. Available from: https://www.sciencedirect.com/topics/engineering/positive-electrode

[12] Heubner C, Langklotz UU, Michaelis MSA. Analysis of the counter-electrode potential in a 3-electrode lithium ion battery cell [Internet]. Sciencedirect.com. 2015 [cited 2022 May 13]. Available from: https://www.sciencedirect.com/science/article/pii/S1572665715301764#:~:text=Lithium%20metal%20is%20used%20as,any%20influence%20of%20the%20CE

[13] Lia Q, Chenb J, Fan L, Kong X, Lu. Y. Progress in electrolytes for rechargeable Li-based batteries and beyond [Internet]. Sciencedirect.com. 2016 [cited 2022 May]. Available from: https://www.sciencedirect.com/science/article/pii/S2468025716300218#:~:text=Most%20of%20the%20electrolytes%20used,(DEC)%2C%20and%2For

[14] Gialampouki MA, Hashemi J, Peterson AA. The electrochemical mechanisms of solid–electrolyte interphase formation in lithium-based batteries. J Phys Chem C Nanomater Interfaces [Internet]. 2019;123(33):20084–92. Available from: https://pubs.acs.org/doi/10.1021/acs.jpcc.9b03886#:~:text=In%20lithium%2Dbased%20batteries%2C%20the,potentials%20inherent%20to%20these%20systems

[15] Liu K, Wang Z, Shi L, Jungsuttiwong S, Yuan S. Ionic liquids for high performance lithium metal batteries [Internet]. Sciencedirect.com. 2021 [cited 2022 May 13]. Available from: https://www.sciencedirect.com/science/article/pii/S2095495620307671

[16] Graz RW. Ionic liquid electrolytes - proionic [Internet]. Proionic.com. [cited 2022 May 13]. Available from: https://proionic.com/ionic-liquids/applications-electrolytes.php?gclid=Cj0KCQjwl7qSBhD-ARIsACvV1X2mOZC2anmG4-tzXrE7nsE0tMMhL5erAGNB-sUkL2iuZkxH-o6GHuMaAup2EALw_wcB

[17] First principles design and investigation of lithium-ion battery cathodes and electrolytes [Internet]. Berkeley.edu. 2011 [cited 2022 Apr]. Available from: https://ceder.berkeley.edu/theses/2011_Shyue_Ping_Ong_Thesis.pdf

[18] Black D. Guide: Lithium-ion battery safety and care [Internet]. Notebookcheck. 2017 [cited 2022 May]. Available from: https://www.notebookcheck.net/Guide-Lithium-Ion-Battery-Safety-and-Care.230968.0.html

[19] Lu X, Pine T, Mumm D, Brouwer J. Modified Pechini synthesis and characterization of Y-doped strontium titanate perovskite. Solid State Ion [Internet]. 2007;178(19–20):1195–9. Available from: https://escholarship.org/content/qt51t0g79c/qt51t0g79c_noSplash_50e95fa26ff3db27c31f4f28bd1956e8.pdf

[20] TWI. What is X-Ray Diffraction Analysis (XRD) and How Does it Work? [Internet]. Twi-global.com. [cited 2022 Apr]. Available from: https://www.twi-global.com/technical-knowledge/faqs/x-ray-diffraction

[21] Dutrow BL. X-ray powder diffraction (XRD) [Internet]. Methods. 2018 [cited 2022 Apr]. Available from: https://serc.carleton.edu/msu_nanotech/methods/XRD.html

[22] Libretexts. Bragg's law [Internet]. Chemistry LibreTexts. Libretexts; 2013 [cited 2022 May 15]. Available from: https://chem.libretexts.org/Bookshelves/Analytical_Chemistry/Supplemental_Modules_(Analytical_Chemistry)/Instrumental_Analysis/Diffraction_Scattering_Techniques/Bragg%27s_Law

[23] Banerjee D. X-Ray Diffraction (XRD) [Internet]. Iitk.ac.in. [cited 2022 Apr]. Available from: https://www.iitk.ac.in/che/pdf/resources/XRD-reading-material.pdf

[24] Omidi M, Vashaee D. Scanning electron microscope. 2017 [cited 2022 Apr]; Available from: https://www.sciencedirect.com/topics/neuroscience/scanning-electron-microscope#:~:text=Scanning%20electron%20microscope%20(SEM)%20is,the%20surface%20of%20the%20sample

[25] BASI. Cyclic Voltammetry - Data Analysis [Internet]. Basinc.com. [cited 2022 Apr]. Available from: https://www.basinc.com/manuals/EC_epsilon/Techniques/CycVolt/cv_analysis

[26] Ossila. Cyclic voltammetry basic principles, theory & setup [Internet]. Ossila. [cited 2022 Apr]. Available from: https://www.ossila.com/pages/cyclic-voltammetry

[27] Peroff A. What is a Potentiostat and how does it work? [Internet]. Pine Research Instrumentation Store. 2021 [cited 2022 Apr]. Available from: https://pineresearch.com/shop/kb/theory/instrumentation/what-potentiostat-does/

[28] Karttunen A. Cyclic voltammetry - solid state chemistry @aalto - aalto university wiki [Internet]. Aalto.fi. 2021 [cited 2022 Apr]. Available from: https://wiki.aalto.fi/display/SSC/Cyclic+voltammetry

[29] Libretexts. 1: Plotting conventions for voltammetry [Internet]. Chemistry LibreTexts. Libretexts; 2016 [cited 2022 May 15]. Available from: https://chem.libretexts.org/Bookshelves/Analytical_Chemistry/Supplemental_Modules_(Analytical_Chemistry)/Analytical_Sciences_Digital_Library/JASDL/Courseware/Analytical_Electrochemistry%3A_The_Basic_Concepts/03_Fundamentals_of_Electrochemistry/B%3A_The_Electrode_Process/01_Plotting_Conventions_for_Voltammetry

[30] Salian A, Mandal S. Entropy stabilized multicomponent oxides with diverse functionality – a review. Crit Rev Solid State Mater Sci [Internet]. 2022;47(2):142–93. Available from: http://dx.doi.org/10.1080/10408436.2021.1886047

[31] Desissa TD, Meja M, Andoshe D, Olu F, Gochole F, Bekele G, et al. Synthesis and characterizations of (Mg, Co, Ni, Cu, Zn)O high-entropy oxides. SN Appl Sci [Internet]. 2021;3(8). Available from: http://dx.doi.org/10.1007/s42452-021-04724-z

[32] Honsberg C, Bowden S. Battery capacity [Internet]. Pveducation.org. [cited 2022 May]. Available from: https://www.pveducation.org/pvcdrom/battery-characteristics/battery-capacity

[33] Bérardan D, Franger S, Dragoe D, Meena AK, Dragoe N. Colossal dielectric constant in high entropy oxides. Phys Status Solidi Rapid Res Lett [Internet]. 2016;10(4):328–33. Available from: http://dx.doi.org/10.1002/pssr.201600043

[34] The first entropy-stabilized complex oxide alloys [Internet]. Anl.gov. [cited 2022 Jun 6]. Available from: https://www.aps.anl.gov/APS-Science-Highlight/2015/The-First-Entropy-Stabilized-Complex-Oxide-Alloys

Appendix 1 Calculations

Calculation of the configurational entropy

M-HEO ($Mg_{0.2}Ni_{0.2}Cu_{0.2}Co_{0.2}Zn_{0.2}O$) with equimolar amount of five different cations. The following equation shows the configurational entropy value of M-HEO.

$$\boldsymbol{S_{config}} = -R\big[\big((x_{Mg}\ln x_{Mg}\big) + (x_{Ni}\ln x_{Ni}) + (x_{Cu}\ln x_{Cu}) + (x_{Co}\ln x_{Co}) + (x_{Zn}\ln x_{Zn})_{cation-cite}) + ((x_O \ln x_O)_{anion-site})\big]$$

$$\boldsymbol{S_{config}} = -R[((0.2\ln 0.2) + (0.2\ln 0.2) + (0.2\ln 0.2) + (0.2\ln 0.2) + (0.2\ln 0.2)_{cation-cite}) + ((1\ln 1)_{anion-site})]$$

$$\boldsymbol{S_{config}} = -R(5 * (0.2\ln 0.2) + 0) = \boldsymbol{1.61R}$$

Calculation of Coulombic efficiency

$$CE = \frac{Charge\ delivered\ during\ discharge}{Charge\ stored\ during\ previous\ charge}$$

Table 5. The result of coulombic efficiency for each 10 cycles.

Number of cycles	Charge delivered during discharge	Charge stored during previous charge	Coulombic efficiency [%]
1	218,333	151,6896	143,9341
2	221,3739	247,7376	89,35821
3	221,3739	257,6736	85,91252
4	223,1984	260,9856	85,52134
5	224,4147	260,9856	85,9874
6	224,4147	264,2976	84,90986
7	227,4556	264,2976	86,0604
8	227,4556	267,6096	84,9953
9	229,2801	270,9216	84,62968
10	230,4964	274,2336	84,05113

Calculation of theoretical & practical capacities

Here presents the theoretical capacity of the active material in anode electrode.

$$Q_{theoretical} = \frac{n*F}{3600*Mw}\ [mAh/g]$$

$$The\ molecular\ weight\ of\ the\ M-HEO\ composition\ is\ 70.1704\ g/mol$$

$$n\ =\ 1Li^{+}\ =\ 1$$

$$F = 96\,485.3321\ s\ A/mol$$

$$Q_{theoretical} = \frac{1 * 96\,485.3321 * 1000}{3600\ * 70.1704} = 381.9485\ [mAh/g]$$

$$Q_{theoretical} \approx 382\ [mAh/g]$$

Here presents the experimental capacity of the active material in anode electrode.

$Q_{experimental} = \frac{I*\Delta t_{cut\ off}}{\Delta V*m}$

$$I = 0.13\ mA$$

$$\Delta t_{cut\ off} = 7511\ s = 2.09\ h$$

$$\Delta V = 3\ V$$

To get the mass of active material in the negative electrode the following calculation was used: (The mass of anode – The mass of pure Al-current collector) * The proportion of the active material) = The mass of active material. (0.0059-0.0044) *0.70 = 0.00105

$$m_{M-HEO} = 0.00105\ g$$

$$Q_{experimental} = \frac{0.13 * 2.09}{0.00105} = \frac{0.2717}{0.00105} = 258.76$$

$$Q_{experimental} \approx 259\ [mAh/g]$$

Appendix 2 Graph

Graph of cyclic voltammetry

Here is the cyclic voltammetry of M-HEO with conventional electrolyte, Platinum as the counter cell and Ag/AgCl as the reference cell.

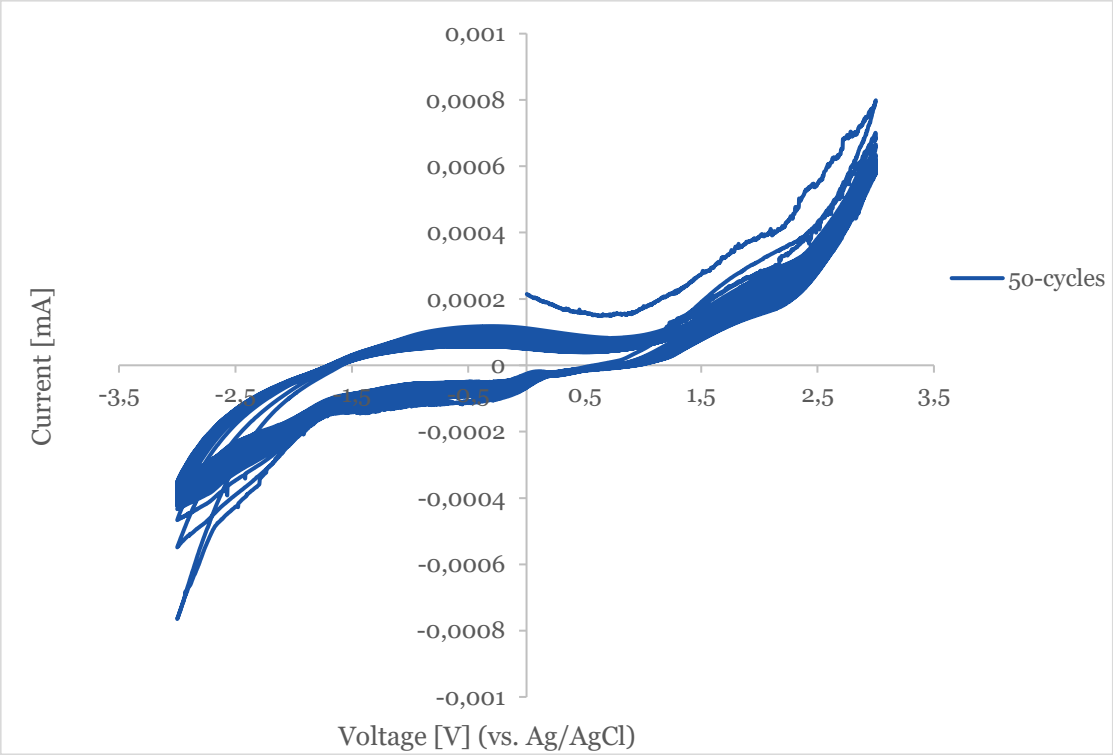

Figure 12. cyclic voltammetry curves of M-HEO.

Graph of Voltage vs time

Here present the charge/discharge curves for the $3Al^{HEO}$ coin cell.

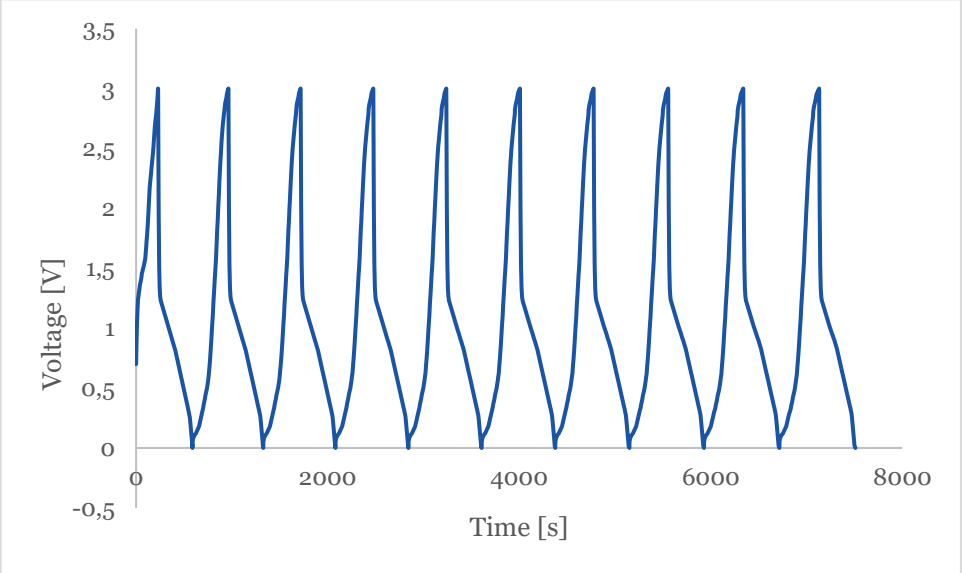

Figure 13. Charge-discharge plot of M-HEO.

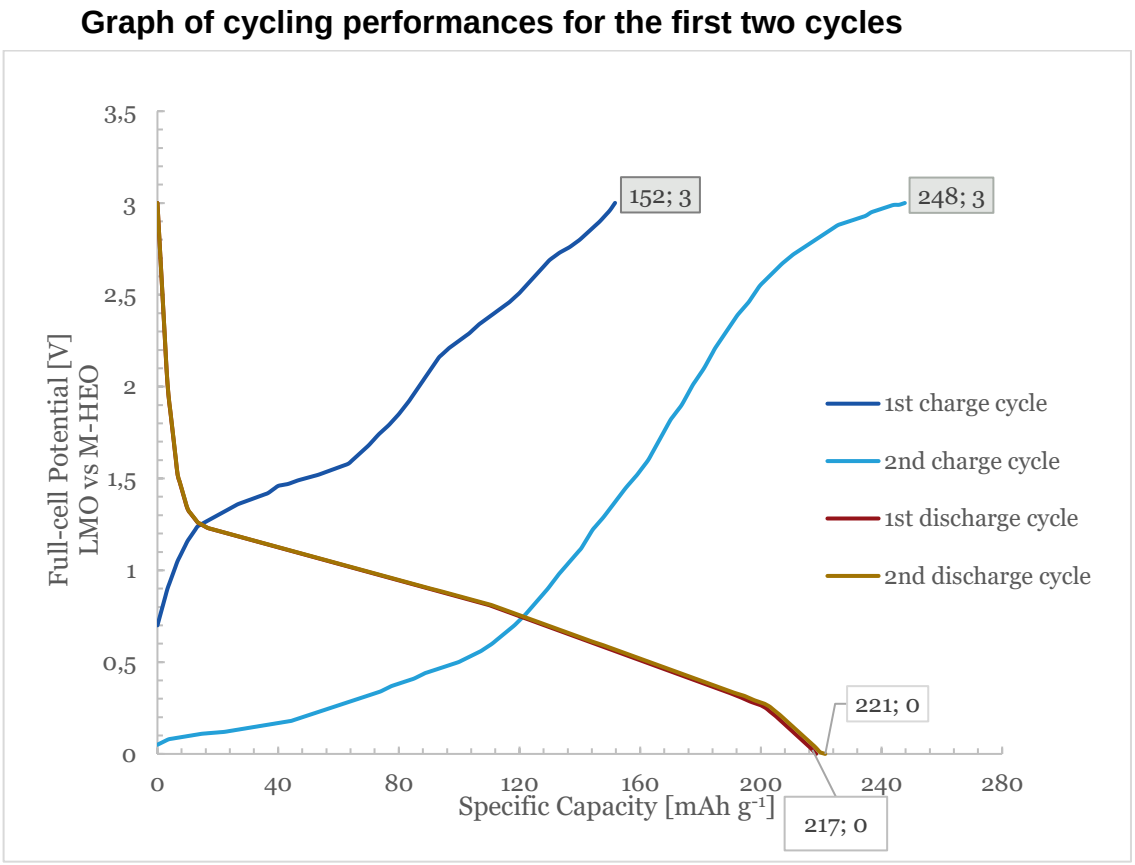

Figure 14. The first and second cycle charge/discharge profiles.